Colloids and Surfaces B: Biointerfaces 134 (2015) 122–130

Contents lists available at ScienceDirect

Colloids and Surfaces B: Biointerfaces

journal homepage: www.elsevier.com/locate/colsurfb

# *In vitro* hematological and *in vivo* immunotoxicity assessment of dextran stabilized iron oxide nanoparticles

Sheeja Liza Easo, Mohanan P.V.*

*Division of Toxicology, Biomedical Technology Wing, Sree Chitra Tirunal Institute for Medical Sciences and Technology, Poojapura, Thiruvananthapuram 695 012, Kerala, India*

ARTICLE INFO

*Article history:*
Received 5 April 2015
Received in revised form 18 June 2015
Accepted 22 June 2015
Available online 29 June 2015

*Keywords:*
Iron oxide nanoparticles
Hemolysis
Platelet aggregation
Lymphocyte proliferation
Cytokines
Intravenous

ABSTRACT

Iron oxide nanoparticles have attracted enormous interest as potential therapeutic agents. The purpose of this study was to examine the *in vitro* hematological toxicity and *in vivo* immune response toward previously synthesized and characterized dextran stabilized iron oxide nanoparticles (DIONPs) developed for hyperthermia application. Peripheral whole blood from human volunteers was used to investigate hemolysis, platelet aggregation, lymphocyte proliferation and cytokine mRNA expression induced by DIONPs *in vitro*. In the concentration range of 0.008–1 mg/ml, DIONPs did not induce relevant levels of hemolysis or platelet aggregation. Assessment of lymphocyte function showed significant suppression of the proliferation activity of T-lymphocytes in cultures stimulated with the mitogen phytohemagglutinin (PHA). In addition, inhibition of PHA-induced cytokine mRNA expressions was also seen. However, systemic administration of DIONPs resulted in enhanced proliferation of mitogen-stimulated spleen derived lymphocytes and secretion of IL-1β at day 7 post exposure. In conclusion, our results demonstrate that immune response is influenced variably by nanoparticles and its degradation milieu. Further investigation of the observed immunosuppressive effects of DIONPs in immune stimulated animal models is required to assess the functional impact of such a response.



## 1. Introduction

Development of nanoparticles for various biomedical applications has greatly increased. This is reflected in the variety of commercialized nanotechnology based products, as well as those in clinical testing for therapeutic and diagnostic purposes. Undoubtedly, the aim in developing nanoparticle based products is to bring considerable benefits to the intended field of application. The potential of nanoparticles to interact with cellular systems owing to its small size and enhanced surface area is widely acknowledged. While such interactions may be beneficial if controlled suitably; conversely, they could result in undesirable toxicity. Intravenous administration of nanoparticles is sure to allow their interaction with blood components, prior to subsequent distribution to tissues and cells.

Preclinical testing of nanoparticles is an essential requirement for any kind of *in vivo* application [1,2]. The surface properties of nanoparticles can greatly affect their compatibility in the bloodstream. On the other hand, blood constituents can react immunologically to render nanoparticles and their drug complexes inactive [3]. RBCs and the multi-component hemostatic cascades, which include platelets and plasma proteins, are crucial in maintaining homeostasis and fluidity of blood in circulation. Hemolytic potential and platelet reactivity has been demonstrated for several nanoparticle preparations [4–7]. Existing reports clearly suggest that nanoparticles interact with immune cells and may cause their stimulation or suppression [8–10]. The ability of nanoparticles to induce an immune response is, in turn, determined by particle size, charge and hydrophobicity. Additionally, it is influenced by several other factors, including the surface targeting moieties, the therapeutic payload, the animal model and the route of administration [11]. Consequently, examination of the hemolytic potential, the platelet aggregation capacity as well as the immune response is crucial to evaluating the toxicity of nanoparticles.

Iron oxide nanoparticles hold immense promise as diagnostic and therapeutic agents in oncology. Their intrinsic physical properties make iron oxide nanoparticles particularly interesting for simultaneous drug delivery, molecular imaging and localized hyperthermia applications. It is well known that iron has immunoregulatory properties, and any alterations in cellular iron levels may affect immune response [12] and inflammatory signaling [13]. Our long-term objective is to use iron oxide nanoparticles as ther-

* Corresponding author.
*E-mail address:* mohanpv10@gmail.com (P.V. Mohanan).

http://dx.doi.org/10.1016/j.colsurfb.2015.06.046
0927-7765/

apeutic agents for hyperthermia treatment; and hence, we have developed dextran stabilized iron oxide nanoparticles (DIONPs) for this purpose. Since the physicochemical properties of nanoparticles are relevant in toxicology and affect their functionality, we had previously performed a complete characterization of DIONPs [14]. In the context of their biomedical application, we consider it crucial to comprehend the outcome of the interactions of DIONPs with blood components that would most certainly come into contact with nanoparticles immediately after systemic absorption. Thus, in this study we report on the interaction of DIONPs with RBCs, platelets and its immunogenic effect on human primary lymphocytes in terms of immunostimulation and immunosuppression, as well as the cytokine response. These investigations are expected to reveal some important elements addressing the toxicity of DIONPs from a preliminary safety standpoint. In addition, we have addressed the delayed immune response in spleen when DIONPs were administered intravenously in rats for a period of 14 days.

## 2. Materials and methods

### 2.1. Materials

Instruments used include dynamic light-scattering (DLS) and zeta-potential analyzer (Zetasizer Nano ZS, Malvern Instruments, Malvern, UK), transmission electron microscope (TEM) (Hitachi H-7650, Japan), fourier transform infrared spectrometer (Nicolet 5700 FTIR, Thermo Electron Corporation, US), microplate reader ($EL_x$808, BioTek, US), automatic hematology analyzer (SYSMEX K4500, Japan), $CO_2$ incubator (MCO-18AIC, Sanyo, Japan), Biophotometer (Eppendorf AG, Hamburg, Germany), iQ5 thermal cycler (Bio-Rad Labortaries, USA) scintillation counter (Triathler, Hidex, Turku, Finland). Chemicals include RPMI-1640 medium, rat tail collagen, lipopolysaccahride (LPS), phytohemagglutinin (PHA), polyethylene glycol (PEG) (Sigma), $Ca^{2+}$/$Mg^{2+}$-free Dulbecco's phosphate-buffered saline (DPBS) (Invitrogen), cyanmethemoglobin (CMH) reagent (Randox Laboratories Ltd., UK), hemoglobin standard (Span Diagnostics Ltd., India), tritiated thymidine [3H] (American Radiolabeled Chemicals, Inc.), Triton X-100 (S D Fine-Chemicals, India), sterile saline (Parenteral Drugs Ltd., India), TRI reagent (Ambion), Quantitative PCR (qPCR) kit (Eurogentec).

### 2.2. Nanoparticles

DIONPs were synthesized and characterized as described previously [14]. Particle core size and morphology were examined using TEM at an accelerating voltage of 80 kV. A drop of the nanoparticle dispersion was deposited on formvar coated grids and air-dried for several hours before analysis. The hydrodynamic radius and polydispersity index (PdI) of nanoparticles was determined using DLS. Samples taken from concentrated nanoparticle (~35 mg/ml) dispersion was diluted in water and complete culture medium to achieve a concentration of 0.05 mg/ml and gently stirred to ensure homogeneity. Appropriate amount of the diluted samples was transferred to disposable cuvettes for analysis. DLS measurements were carried out at 25 °C, at a scattering angle of 173°. The Z-average intensity-weighted radii were calculated using the instrument software. Zeta potentials of freshly prepared 0.05 mg/ml nanoparticle dispersions in water and complete culture medium were also measured at 25 °C. All measurements were calculated as an average of three runs containing 12 measurements per run after 4 h incubation. To evaluate dextran coating on nanoparticle surface and the nature of its bonding, FTIR analysis was performed. Briefly, freeze dried nanoparticle preparations were mixed with potassium bromide to form a fine powder. The powder was compressed into a thin pellet, and the FTIR spectrum was recorded between 4000 $cm^{-1}$ and 400 $cm^{-1}$ at a resolution of 4 $cm^{-1}$.

Nanoparticle concentration was expressed as mg of Fe per ml in all experiments. For cell exposure experiments, DIONPs dispersion in varying concentrations ranging from 0.008–1 mg/ml was freshly prepared by diluting the DIONPs suspension in the appropriate medium.

### 2.3. In vitro *studies*

#### 2.3.1. Subjects

A total of six volunteers participated in this study (male and female). Blood was collected by venipuncture into tubes containing appropriate anticoagulants. Blood samples obtained from participants were pooled for all experiments. Study participants signed an informed consent form, and the study was approved by the Institutional Ethics Committee (ECR/189/Inst/KL/2013).

### 2.4. Hemolysis assessment

Hemolysis assay was performed as described in http://ncl.cancer.gov/NCL_Method_ITA-1.pdf. Briefly, blood samples were collected into vials with heparin as the anticoagulant. The total hemoglobin concentration of heparinized human whole blood was measured using cyanmethemoglobin method based on a hemoglobin standard curve at an absorbance wavelength of 540 nm. Blood was diluted to obtain a final hemoglobin concentration of 10 mg/ml with $Ca^{2+}$/$Mg^{2+}$ free DPBS. Nanoparticle samples at four different concentrations (0.008. 0.04, 0.2 and 1 mg/ml) along with positive (Triton X-100) and negative controls (PEG) were analyzed. Aliquots (100 μl) of the nanoparticle suspension were added to microcentrifuge tubes, followed by the addition of 700 μl of $Ca^{2+}$/$Mg^{2+}$ free DPBS. To each of these tubes, 100 μl of diluted blood was added. Tubes were incubated in a 37 °C water bath for 3 h, with gentle inversion of the sample tubes every 30 min. Following incubation, tubes were centrifuged at 800× *g* for 15 min at room temperature. The supernatant was mixed in a 1:1 ratio with CMH reagent and analyzed at 540 nm in a microplate reader. Sample absorbance was corrected for background interference (particles in DPBS without blood). The concentration of cell-free hemoglobin in each sample was assessed from the hemoglobin standard curve by accounting for the 16-fold dilution factor for samples and controls. Finally, percentage hemolysis was obtained by dividing each sample's cell-free hemoglobin concentration by total hemoglobin concentration (10 mg/ml).

### 2.5. Evaluation of platelet aggregation

To study the effect of nanoparticles on platelet aggregation, whole human blood collected in vials containing sodium citrate anticoagulant was centrifuged for 8 min at 200× *g* to obtain platelet rich plasma (PRP). This PRP was treated separately with DIONPs (0.008, 0.04, 0.02 and 1.0 mg/ml), PBS (negative control) and collagen (positive control) for 15 min at 37 °C. To investigate whether DIONPs could interfere with collagen-induced platelet aggregation, PRP was also treated with a mixture of collagen and DIONPs under the same conditions. A single-platelet count was then conducted using an automatic hematology analyzer. A decrease in single platelet count due to platelet aggregation was used to calculate percentage aggregation. A detailed protocol is available at http://ncl.cancer.gov/NCL_Method_ITA-2.pdfhttp://ncl.cancer.gov/NCL_Method_ITA-2.pdf

**Table 1**
PCR primers for cytokine expression

| S. No. | Genes | Sequences | Accession No. | $T_m$ | bp |
|---|---|---|---|---|---|
| 1 | IL-1β | F-ATAAGCCCACTCTACAGCT<br>R-ATTGGCCCTGAAAGGAGAGA | NM000576.2 | 60 °C | 442 |
| 2 | IL-4 | F-ACTGCTTCCCCCTCTGTTCTTC<br>R-GTACTGTGGTTGGCTTCCTTCAC | NM000589.3 | 60 °C | 378 |
| 3 | IL-6 | F-CAGCCACTCACCTCTTCAGAAC<br>R-TGCAGGAACTGGATCAGGAC | NM000600.3 | 60 °C | 332 |
| 4 | IL-10 | F-ATGCCCCAAGCTGAGAACCAAGAC<br>R-TCTCAAGGGGCTGGGTCAGCTATCCCA | NM000572.2 | 66 °C | 352 |
| 5 | TNF-α | F-CAGAGGGAAGAGTTCCCCAG<br>R-CCTTGGTCTGGTAGGAGACG | NM000594.3 | 63 °C | 325 |
| 6 | β-actin | F-CTGGGACGACATGGAGAAAA<br>R-AAGGAAGGCTGGAAGAGTGC | NM001101.3 | 53 °C | 564 |

## 3. Immunological assessment

### 3.1. Isolation of lymphocytes

Peripheral blood lymphocytes were isolated using Histopaque-1077 solution following a standardized protocol. Briefly, blood was diluted with DPBS in a 1:1 ratio, layered over Histopaque-1077 and centrifuged at 900× *g*, 18–20 °C for 30 min. The upper layer containing plasma and platelets was removed and discarded. The mononuclear cell layer containing lymphocytes in the interface between the plasma layer and the RBC-granulocyte layer was carefully transferred to another tube, and washed with excess volume of DPBS twice. Finally, lymphocytes at a density of $1 \times 10^6$ cells were resuspended in RPMI-1640 medium supplemented with 10% heat inactivated FBS, 2 mM glutamine, 100 U/ml penicillin and 100 mg/ml streptomycin (complete culture medium). Viability and cell count was determined using trypan blue staining. The range of viable cells was always >90%. Cultures were incubated at 37 °C and 5% $CO_2$ atmosphere.

### 3.2. Analysis of lymphocyte proliferation response

Assessment of lymphocyte proliferation was performed as described in http://ncl.cancer.gov/NCL_Method_ITA-6.pdf with slight modifications. $1 \times 10^5$ cells were placed in a 96-well microplate in 200 μl aliquots, and exposed to increasing concentrations of DIONPs (0.008. 0.04, 0.2 and 1 mg/ml) in the presence and absence of mitogen PHA (2.5 μg/ml). The wells receiving DPBS was regarded as negative control, while those receiving PHA was considered as positive control. Cells were cultured for 48 h at 37 °C, 5% $CO_2$ atmosphere. The cultures, excluding negative control wells, were pulsed with [3H] thymidine (1 μCi/well) for the last 24 h. At the end of 72 h, cells were harvested and the amount of radioactivity incorporated into cellular DNA was measured using a scintillation counter. [3H] thymidine uptake was expressed as mean counts per minute (cpm). The lymphocyte proliferation levels were calculated by subtracting mean cpm of nanoparticle treated sample from that of negative control, whereas the level of proliferation inhibition was obtained by dividing the difference between mean cpm of positive control samples and that of positive control plus nanoparticles treated samples by mean cpm of positive control. Results were expressed as percentage of respective controls.

### 3.3. Quantification of cytokine expression

Cytokine expression was quantified by real time qRT-PCR. Total RNA was isolated from lymphocytes exposed to 1 mg/ml DIONPs for 24 h using TRI reagent, according to the manufacturer's protocol. RNA concentration was estimated by measuring the absorbance at 260 nm using a Biophotometer. RNA samples were kept frozen at −80 °C until use. RNA (200 ng) was reverse transcribed into complementary DNA using the reverse transcriptase core kit, according to the manufacturer's instructions. Expression of the following cytokines was analyzed: IL-1β, 1L-4, IL-6, IL-10 and TNF-α. Primer sequences of all genes are given in Table 1. Polymerase chain reactions were performed in a thermal cycler using the following amplification program: an initial period of 10 min at 95 °C, 40 cycles of 15 s denaturation at 95 °C, 20 s annealing at 53–66 °C, and finally 40 s extension at 72 °C. The program was terminated with 10 min at 72 °C. β-actin (ACTB) was used as the internal reference gene for normalizing the expression data. Amplification of genes was analyzed by continuously monitoring the fluorescence of each sample *vs.* cycle numbers, and threshold cycle (Ct) values were calculated by the iQ5 optical system software, version 2.1. Product specificity was monitored by melting curve analysis.

### 3.4. In vivo *studies*

#### 3.4.1. Animals and treatment

Male Wistar rats 10–12 weeks old with an average body weight of 200–220 g were housed in polysulfone cages with stainless steel mesh in a well-ventilated room. The room was maintained at 22 ± 2 °C, 30–70 ± 10% relative humidity and a 12 h light/dark cycle. Rats were given pellet feed and sterilized water. Animals were acclimatized for a period of 5 days before experimentation, and all procedures complied with the guidelines of institute animal ethics committee (IAEC) regulations approved by committee for the purpose of control and supervision of experiments on animals (CPCSEA), Govt. of India (2422012 II–VI).

For analysis of lymphocyte proliferation and cytokine response, twelve rats were randomly divided into two groups (7 and 14 days), with three controls and three treated animals in each group. Control rats were injected intravenously with sterile saline, whereas test rats were administered with the test substance preparation containing DIONPs at a dose of 10 mg/kg body weight. At the end of the designated period, rats were anesthetized by ether and blood samples were collected from the orbital sinus of animals for cytokine analysis. Rats were then sacrificed by cervical dislocation and spleen tissue was collected for further assay.

### 3.5. Preparation of spleen-derived lymphocytes

Individual spleens were dispersed mechanically on steel mesh in DPBS, pH 7.4 to obtain splenocyte suspensions, which were filtered through 0.45 μm nylon cell strainer to remove large clumps. These suspensions were layered over Histopaque-1077 solution and lymphocytes were separated as previously described. Cell density was adjusted to $1 \times 10^6$ cells/ml for further assay.

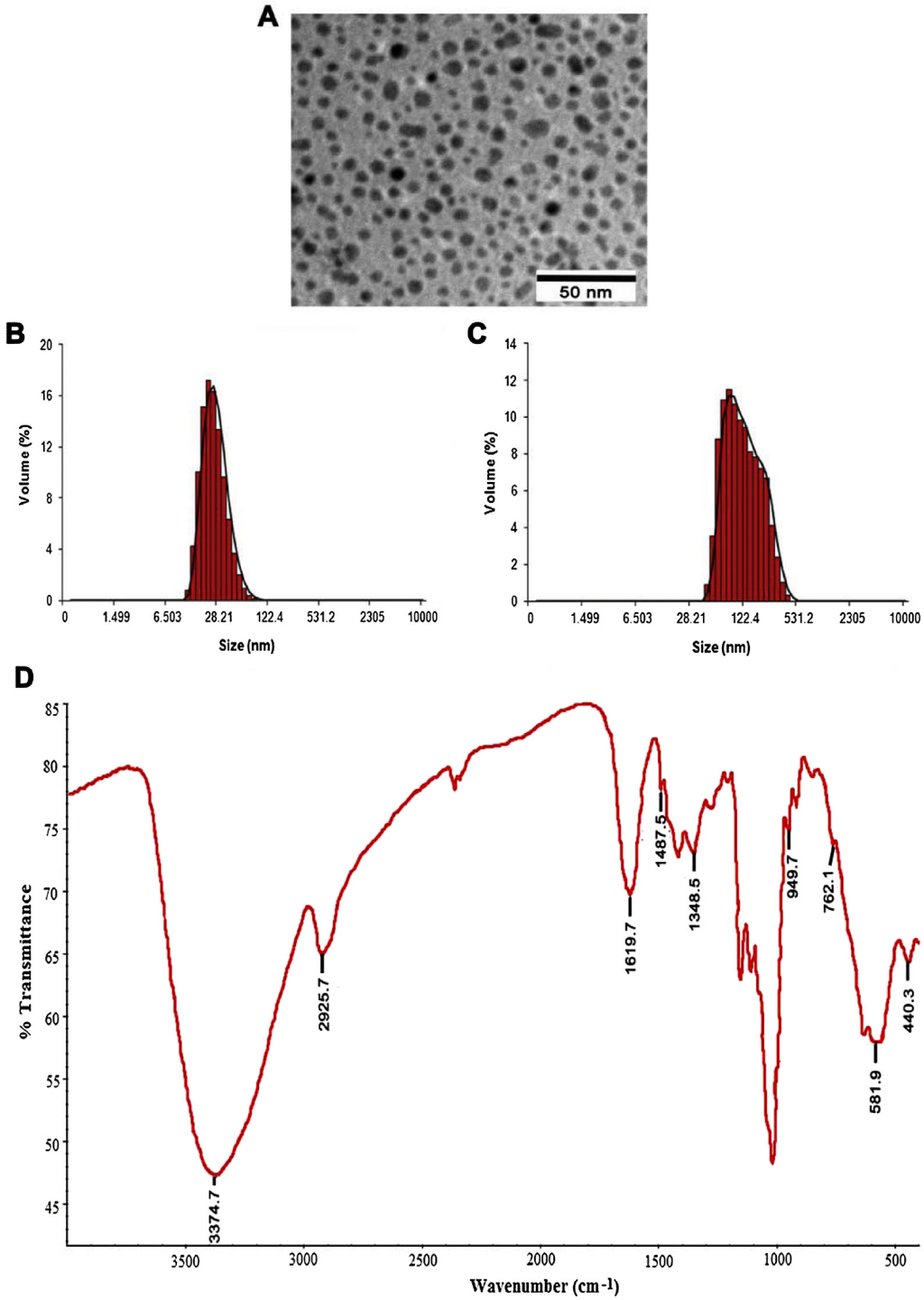


**Fig. 1. Physicochemical characterization of nanoparticle.** (A) TEM analysis indicates DIONPs to be spherical in shape with an average core diameter of 9 nm. (B) The mean hydrodynamic size of DIONPs measured by DLS in water was 25 nm. (C) The mean hydrodynamic size of DIONPs in culture medium was 123 nm. (D) FTIR analysis was used to demonstrate dextran coating on the surface of iron oxide nanoparticles.

### 3.6. Mitogen-stimulated lymphocyte proliferation response

Lymphocyte proliferation response to mitogens (PHA and LPS) was evaluated using the [3H] thymidine incorporation assay. Lymphocyte suspensions from spleen of each treated animal were placed in a flat-bottom 96-well plate in 100 μl aliquots. Cells at a density of $1 \times 10^5$ cells/ml was respectively introduced with T-cell mitogen (PHA, 5 μg/ml, 100 μl per well, three wells for each animal) and B-cell mitogen (LPS, 10 μg/ml, 100 μl per well, three wells for each animal). Meanwhile, wells receiving complete RPMI-1640 medium were regarded as controls. The plate was incubated at 37 °C, 5% $CO_2$ for 48 h and the remaining procedure was performed as described earlier. Lymphocyte proliferation response was expressed in terms of stimulation index (SI), which was calculated by dividing mean cpm of stimulated cultures by mean cpm of unstimulated cultures.

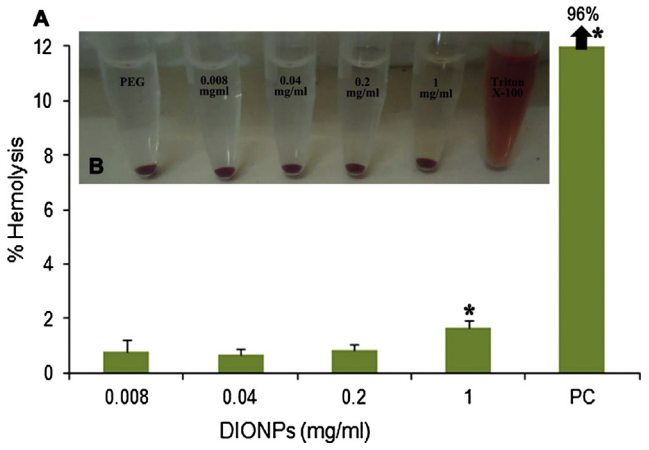


**Fig. 2.** ***In vitro*** nanoparticle-induced hemolysis. (A) Percentage hemolysis induced by DIONPs did not exceed the 5% damage criterion listed in the ASTM E2525-08 standard. PEG was used as negative control, NC and Trition X-100 was used as positive control, PC. Results expressed as mean ± SD ($n = 6$). (B) Pictographic representation of hemolysis in samples treated with PEG, DIONPs and Triton X-100.
*signifies $p < 0.05$ compared to control.

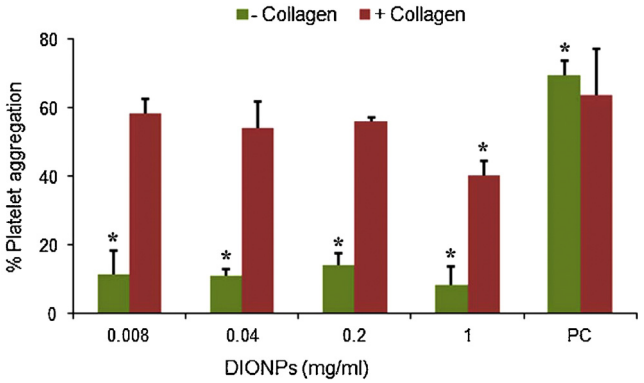


**Fig. 3.** ***In vitro*** platelet aggregation. Under the tested conditions platelet aggregation induced by DIONPs was within the 20% assay threshold. But a significant decrease in collagen-induced platelet aggregation was observed at the highest concentration (1 mg/ml). PC, positive control (collagen). Results expressed as mean ± SD ($n = 4$).
*signifies $p < 0.05$.

### 3.7. Cytokines analyses in blood

Serum samples were obtained from blood by centrifugation at 3000 rpm for 10 min at 4 °C and immediately frozen at −20 °C for further detection. IL-1β, IL-6 and TNF-α secretion in serum was measured using commercially available ELISA kits (Thermo Scientific, US), according to the manufacturer's instructions.

### 3.8. Statistical analysis

Data was expressed as mean ± standard deviation (SD). The difference of means among groups was analyzed by one-way analysis of variance (ANOVA) method. For statistical analysis, each of the experimental values was compared to its corresponding control using Student's *t*-test. Statistical significance was set at $p < 0.05$.

## 4. Results

### 4.1. Nanoparticles

TEM analysis revealed that synthesized nanoparticles had an average core diameter of 9.08 ± 1.48 nm. The mean volume hydrodynamic size of particles in water was 25.3 ± 0.97 nm. The Z-average intensity-weighted hydrodynamic radius of DIONPs was 38.68 ± 0.96 nm and PdI, which is a measure of the width of the nanoparticle size distribution was 0.2. DLS measurements of DIONPs in complete culture medium indicated the hydrodynamic size to be 123.1 ± 6.48 nm. The Z-average hydrodynamic radius was 119.1 ± 7.74 with a PdI value of 0.1. The zeta potential of particles measured in water (pH 7) and culture medium (pH 7.4) was −7.87 mV and −11.6 mV, respectively. The mean size of particles suspended in culture medium was higher than the mean size of particles in water, indicating that particles tend to form larger complexes in culture medium. However, the zeta potential of DIONPs was not significantly affected in culture medium. FTIR analysis provided details about dextran coating and bonding on the nanoparticle surface, and has been previously discussed elsewhere [14] (Fig. 1).

### 4.2. In vitro *studies*

#### 4.2.1. Nanoparticle-induced hemolysis

The degree of hemolysis caused by DIONPs exposed to diluted blood for 3 h as shown in Fig. 2A. The percentage hemolysis observed with 0.008, 0.04, 0.2 and 1 mg/ml DIONPs was 0.77%, 0.66%, 0.83% and 1.68%. At the highest concentration, the percentage hemolysis was slightly yet significantly increased in comparison to control. According to the criterion in the ASTM E2524-08 standard, percentage hemolysis > 5% indicates that the test material causes damage to RBCs; however, this criterion was not exceeded at any of the particle concentrations. As presented in Fig. 2B, Triton X-100 caused perceptible lysis of RBCs, but DIONPs was not visibly hemolytic at any of the tested doses.

### 4.3. Nanoparticle-induced platelet aggregation

Platelet aggregation was measured in the presence and absence of agonist collagen. DIONPs increased platelet aggregation, to some extent (8–14%) across all concentrations; however, the percentage increase was within the 20% assay threshold. In the presence of collagen, there was a significant decrease in platelet aggregation (15%) at the highest concentration of DIONPs compared to collagen treated control cells (Fig. 3).

### 4.4. Lymphocyte proliferation response

The possible effect of DIONPs on lymphocyte proliferation response was assessed by exposing lymphocytes to increasing concentrations of nanoparticles for 72 h and analyzing the proliferation response using [3H] incorporation. While PHA induced a significant increase in lymphocyte proliferation (90.25%) (Fig. 4A and D) compared to control (DPBS) (Fig. 4A and B), DIONPs exposed cells showed only a minimal increase in levels of lymphocyte proliferation (3–6%) (Fig. 4A and C). The aggregation seen in nanoparticles exposed cultures was due to the formation of particle aggregates in culture medium (Fig. 4C), as indicated by an increase in hydrodynamic size of particles.

Immunosuppression by nanoparticles is another major concern because of the possible cytotoxicity to immune cells. In order to assess whether DIONPs interferes with the normal proliferative capacity of lymphocytes in response to mitogen, lymphocytes were exposed to DIONPs in the presence of PHA for 72 h. The results indi-

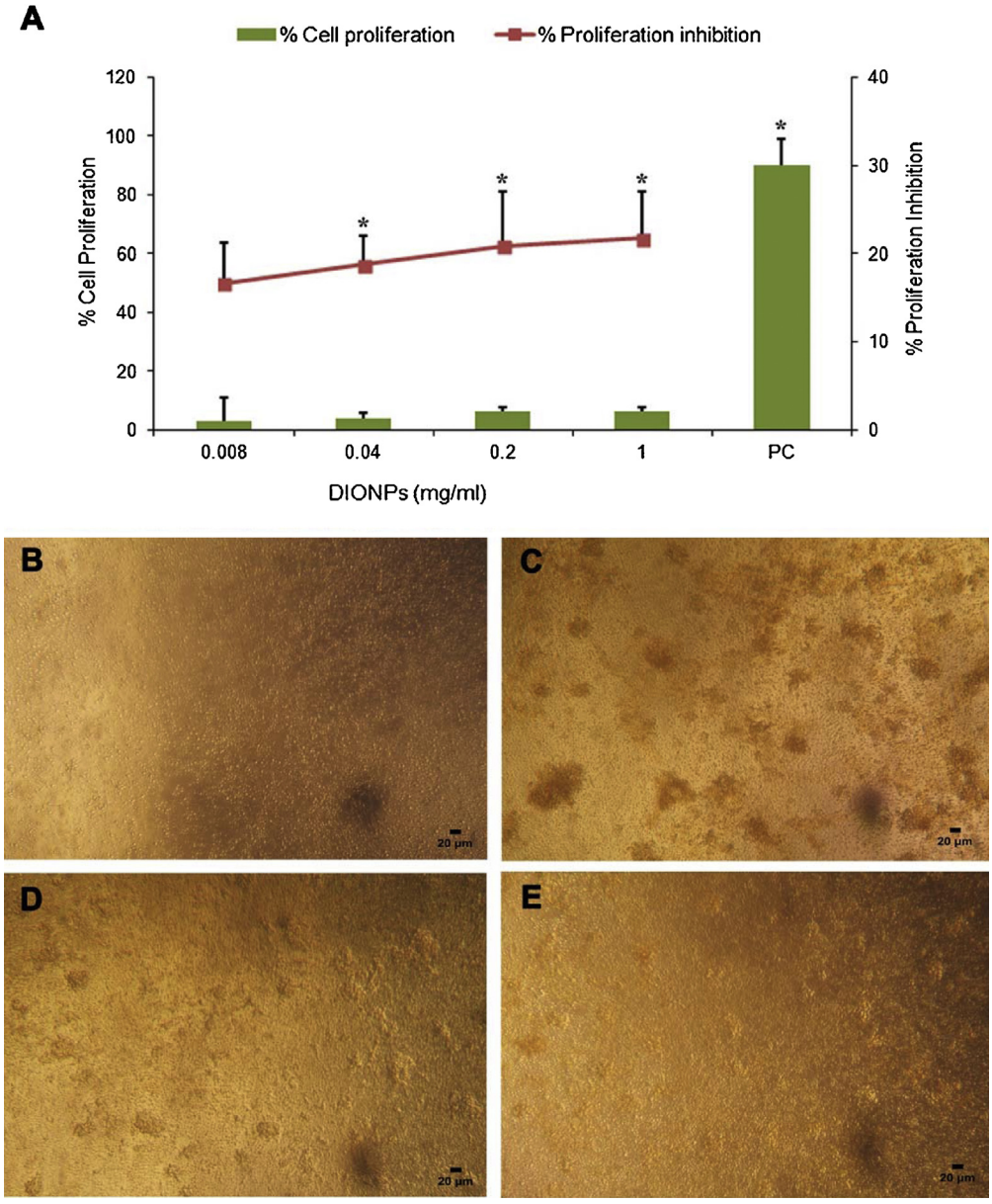


**Fig. 4.** ***In vitro*** lymphocyte proliferation response. (A) DIONPs did not induce significant levels of proliferation in human peripheral blood lymphocytes. However, a dose-dependent inhibition of PHA-induced lymphocyte proliferation was observed. Results expressed as mean ± SD ($n = 6$). (B) Phase contrast micrographs of lymphocytes treated with DPBS (Dulbecco's Phosphate buffered saline). (C) Lymphocytes treated with DIONPs. The dark clusters observed are not proliferated cells; rather they indicate NPs that have aggregated in the culture medium. (D) Lymphocytes treated with PHA. (E) PHA stimulated lymphocytes treated with DIONPs. PC, positive control (PHA).
*signifies $p < 0.05$.

cate that DIONPs caused a dose-dependent increase in inhibition of PHA-induced lymphocyte proliferation (16–21%) (Fig. 4A and E).

### 4.5. Cytokine expression

Next, the expression of a panel of cytokines, including IL-1β, IL-4, IL-6, IL-10 and TNF-α was assessed by qRT-PCR following 24 h of lymphocyte exposure to 1 mg/ml DIONPs. The expression level of IL-4 was increased by 1.5 fold relative to control cells, which is indicative of a Th2 type response. Under the condition of PHA incubation, the expressions of IL-4, IL-10 and TNF-α was enhanced, while IL-1β expression was substantially decreased. Co-incubation of stimulated lymphocytes with DIONPs decreased the expression of all cytokines that were enhanced by PHA (Fig. 5).

### 4.6. In vivo *studies*

#### 4.6.1. Ex vivo *mitogen-stimulated lymphocyte proliferation response*

Mitogens PHA and LPS were used to differentiate the proliferation response of spleen derived T- and B-lymphocytes, respectively (Fig. 6). In response to DIONPs, both T- and B-lymphocyte proliferation registered a significant increase on day 7. However, the proliferation capacities in both T- and B-lymphocyte populations were comparable to respective controls on day 14 post exposure.

### 4.7. Analysis of cytokines in blood

The effect of DIONPs on the release of three proinflammatory cytokines, namely IL-1β, IL-6 and TNF-α was examined in blood serum using commercially available ELISA kits. DIONPs exposure

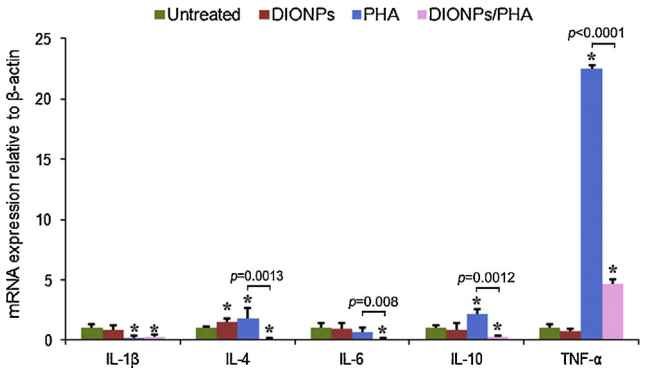


**Fig. 5.** ***In vitro*** cytokine expression in lymphocytes. In unstimulated lymphocytes DIONPs enhanced the expression of IL-4. Enhanced expression of IL-4, IL-10 and TNF-α mRNA occurred in PHA exposed cultures. DIONPs caused the suppression of all cytokines whose expressions were enhanced by PHA at 24 h. Results expressed as mean ± SD ($n = 3$). $p$-values (one-way analysis of variance, ANOVA) denoting significant differences between PHA and DIONPs/PHA treated cultures are provided in the graphs.
* signifies $p < 0.05$ in comparison to untreated control cultures.

significantly increased the level of IL-1β on day 7, while no effect was observed on day 14 after treatment (Fig. 7A). Additionally, no significant alteration was seen in IL-6 and TNF-α secretion at any of the time points considered (Fig. 7B and C).

## 5. Discussion

The determination of hemolyis is based on the spectrophotometric detection of hemoglobin and is an extremely sensitive technique, which has been exploited in several studies [15,16]. Our hemolysis result is in agreement with previous studies that have reported on the non-hemolytic properties of polymer coated iron oxide nanoparticles [17,18]. The mechanism behind this lack of DIONPs-induced hemolysis is probably due to the presence of dextran layer on nanoparticle surface, since dextran coating has been shown to prevent adhesion of nanoparticles to RBC membrane [19]. Another factor that may contribute to the non-hemolytic property of DIONPs is its propensity to form specific interactions with plasma proteins [20]. Formation of a plasma protein corona on NP surface has been shown to protect red blood cells from nanoparticles-mediated hemolysis [21,22].

The potential effect of DIONPs on platelet function was assessed using light transmission aggregometry. DIONPs did not induce relevant levels of platelet aggregation, although collagen-induced platelet aggregation was inhibited at 1 mg/ml concentration

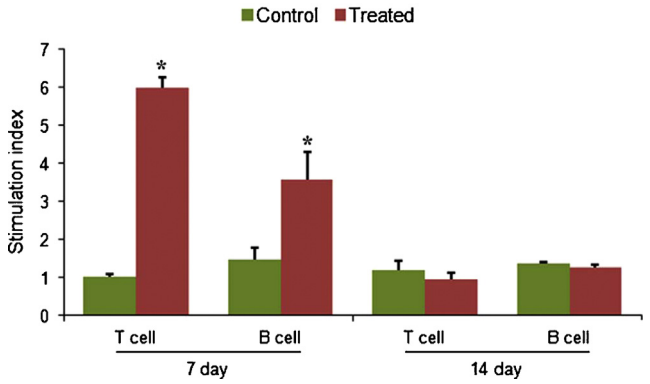


**Fig. 6. Mitogen stimulated lymphocyte proliferation response in rat spleen.** DIONPs increased the proliferation of both T and B lymphocytes at day 7 after a single intravenous administration of NPs. Results expressed as mean ± SD ($n = 3$).
*signifies $p < 0.05$.

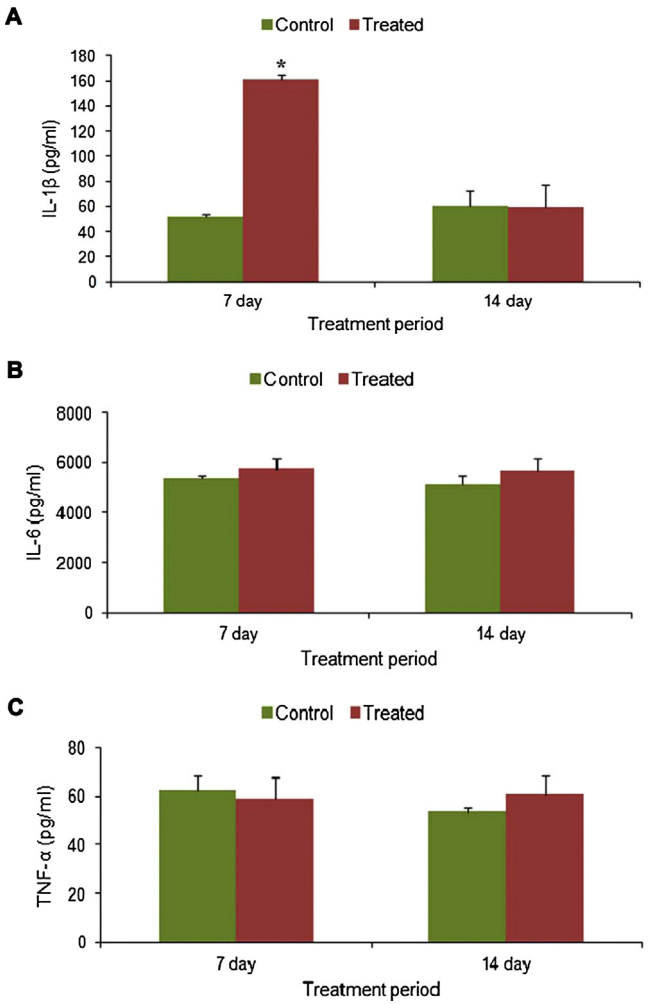


**Fig. 7. Cytokine secretion in serum of rats.** (A) A single intravenous dose of 10 mg/kg DIONPs resulted in increased secretion of IL-1β cytokine at day 7 of exposure. The secretion of IL-6 (B) and TNF-α (C) were not affected at any of the time points considered. Results expressed as mean ± SD ($n = 3$).
*signifies $p < 0.05$.

in comparison with control. Available literature reports varied platelet responses for iron oxide nanoparticles with different surface functionality. For example, citric acid functionalized iron oxide nanoparticles was shown to possess anti-platelet activity, while starch coated iron oxide nanoparticles behaved neutrally [23]. The polymer dextran has been shown to possess anti-thrombotic and anti-platelet function [24]. A few studies have previously reported on the ability of dextran to reduce agonist induced platelet aggregation [25,26]. Platelets absorb dextran, with resultant changes in electrophoretic mobility; suggesting that the inhibitory effect of dextran on platelet function might be due to some alteration of platelet membrane function [27]. Other findings suggest that dextran may temporarily impair platelet function by interfering with factor VIII [28]. Additionally, the inhibitory effect of dextran infusions on platelet function were shown to be dose-related [29]. With higher concentration of DIONPs, it is probable that platelets would be exposed to greater amounts of surface dextran moieties, resulting in reduced collagen-induced platelet aggregation.

Lymphocyte proliferation is one of the central aspects of cellular immunity, and cytokines are important mediators in the regulation of immune responses. The results of this study demonstrate that although exposure to DIONPs did not excessively influence the proliferation of resting lymphocytes (immunostimulation), the expression of IL-4, a typical Th2-cell derived cytokine was

enhanced. Generally, resting or unstimulated lymphocytes does not produce or secrete cytokines and only express or release cytokines following activation [30,31]. Therefore, it is probable that while the levels of lymphocyte proliferation induced by DIONPs were not statistically relevant compared to controls, it appears to have been sufficient to cause increased expression of IL-4. Although the significance of this nanoparticle-induced IL-4 response is not clear, it is possible that a Th2 type response would favor antibody production [32]. The possibility of suppression of lymphocyte proliferation by DIONPs was assessed in PHA-stimulated cultures. Significant level of proliferation inhibition was observed in PHA-stimulated lymphocytes, which was not related to direct cytotoxicity, since the viability of lymphocytes in all cultures was >90%. A relevant point that needs to be considered involves the possibility of dextran coating on DIONPs to interact with PHA, since PHA has an affinity for carbohydrates. However, it should be noted that lectin proteins have carbohydrate specificity. The specificity of PHA is directed toward complex oligosaccharides containing galactose, *N*-acetylglucosamine and mannose moieties [33]. Hence, the proliferation inhibition induced by DIONPs appears to be particle-specific, and is not due to interaction of PHA with the dextran coating of nanoparticles. In addition to inhibition of lymphocyte proliferation, DIONPs also caused a reduction of PHA-induced cytokine expression indicating a potential for DIONPs to induce immunosuppression of PHA activity in lymphocytes. PHA specifically induces proliferation of T-lymphocytes in human peripheral blood via T-lymphocyte membrane receptor, directly without the need for antigen presenting cells [34]. Thus, it may be plausible that DIONPs may interfere with PHA-induced signal transduction via lymphocyte membrane receptors. Studies related to immunotoxicity of iron oxide nanoparticles toward T-cell reactivity are very rare. One such study by Sundstrom et al. showed that rhesus macaque T-cells labeled with monocrytalline iron oxide nanoparticles resulted in the uptake of these particles within the cytoplasm, with no relevant effects seen on resting or activated lymphocyte proliferation and cytokine responses [35]. *In vitro* immunotoxicity evaluation with other nanoparticles such as hydrophobic sodium fluoride-based nanocrystals doped with lanthanide ions showed significant suppression of the proliferation activity of T-lymphocytes and T-dependent B-lymphocytes in peripheral blood cultures stimulated with mitogens [36]. Lankoff et al. reported a dose-dependent decrease in the proliferation status of T-lymphocytes with increasing concentrations of different types of silica nanoparticles. Moreover, it was demonstrated that this effect was induced as a result of inhibition of the cell cycle progression from G1 to S phase [37].

*In vitro* models serve as tools to evaluate the cellular mechanisms related to exposure of nanoparticles, but *in vivo* models are better suited to provide insight into the toxic effects of nanoparticles, considering the numerous interactions of different cell types and multiple organ systems. Previous studies have established that iron oxide nanoparticles administered systemically accumulates in spleen, where they are subsequently degraded into ferrous and ferric iron, which are then incorporated into the hemoglobin of erythrocytes and various iron binding proteins [38,39,40,41]. Chen et al. reported that low concentrations of iron oxide nanoparticles enhanced the proliferation of splenic T-cells in ICR mice [42]. In one of our studies, wherein the biodistribution of a single dose of DIONPs was investigated, we observed increased distribution of iron in spleen ranging from 24 to 166% of control corresponding to a period of 1–14 days, indicating that spleen was a major storage organ for DIONPs degradation products (Easo and Mohanan, unpublished results). In this context, we analyzed the effect of DIONPs on the delayed lymphocyte proliferation response at days 7 and 14. DIONPs had a significant effect on T-cell activity as indicated by the increased proliferation of T-lymphocytes after PHA stimulation of spleen cells. B-cell activity was also affected as indicated by the enhanced proliferation of B-cells, and increase in IL-1β secretion after LPS stimulation of spleen cells. Surprisingly, the effect of DIONPs on lymphocyte reactivity was not extended to day 14. Hence, the observed immune response toward DIONPs at the earlier time point may be a normal biologic response to the accumulation of iron, which was limited to the duration of one week.

It is obvious that there is an overall discrepancy between the *in vitro* and *ex vivo* lymphocyte proliferation data based on [3H] incorporation. It is noteworthy that systemic administration of iron oxide nanoparticles will undoubtedly result in their degradation into molecular iron metabolites over time. Hence, the observed *ex vivo* result may invariably be a manifestation of spleen response to DIONPs degradation and clearance. On the contrary, the results of the *in vitro* proliferation response do not account for nanoparticles biodistribution and may reflect the potential of DIONPs to cause immunosuppression upon direct interaction. Indeed, Shen et al. demonstrated that systemic exposure to a single dose of iron oxide nanoparticles suppressed subsequent antigen-specific immune reactions, including the serum production of antigen-specific antibodies and the functionality of T-cells [43]. The demonstration of mitogen-specific lymphocyte suppression by DIONPs in our *in vitro* study needs to be further investigated in immune stimulated *in vivo* models to evaluate the functional impact of such suppression.

## 6. Conclusion

Based on the results of the *in vitro* hematological assessment, a preliminary conclusion could be drawn that DIONPs exerted a certain degree of immune modulation by inhibition of mitogen-stimulated lymphocyte proliferation as well as suppression of mitogen mediated cytokine expression. The observed functional changes indicate that T-lymphocytes may revert to a less responsive state with DIONPs treatment. Such a lymphocyte response may be beneficial for the induction of tolerance in clinical conditions such as allergic diseases. However, this *in vitro* response needs to be corroborated and confirmed using *in vivo* models, before it can be effectively concluded. In a more a realistic context, systemic administration of a single dose of DIONPs resulted in enhanced spleen derived lymphocyte proliferation response accompanied by the production of IL-1β cytokine. This delayed immune effect was limited to a period of one week. Thus, successful utilization of DIONPs for therapeutic purposes requires further evaluation of its interaction with key immune cells such as macrophages and dendritic cells, and downstream immune processes such as the complement pathway.

## Declaration of interest/disclosure

The authors report no conflict of interest in this work.

## Acknowledgements

The authors are grateful to the Director of Sree Chitra Tirunal Institute for Medical Sciences and Technology and Head of Biomedical Technology Wing for their support. The authors acknowledge the financial support provided by the Department of Science and Technology, India (Grant No. SR/NM/NS-90/2008). Technical assistance from Ms. Legi B, Mr. Renjith Kartha and the assistance of Mr. Shaji S and Mr. Harikumar G during the *in vivo* experiments are greatly appreciated. Sheeja Liza Easo acknowledges the Council of Scientific and Industrial Research (CSIR), New Delhi, India, for financial support.

## References


[1] M.A. Dobrovolskaia, P. Aggarwal, J.B. Hall, S.E. McNeil, Mol. Pharm. 5 (2008) 487.
[2] M.A. Dobrovolskaia, S.E. McNeil, J. Control. Release 172 (2013) 456.
[3] S. Naahidi, M. Jafari, F. Edalat, K. Raymond, A. Khademhosseini, P. Chen, J. Control. Release 166 (2013) 182.
[4] M.J. Kim, S. Shin, Food Chem. Toxicol. 67 (2014) 80.
[5] H. Zheng, J. Liu, L. Du, Nanoscale 6 (2014) 9017.
[6] M. Šimundić, B. Drašler, V. Šuštar, J. Zupanc, R. Štukelj, D. Makovec, D. Erdogmus, H. Hägerstrand, D. Drobne, V. Kralj-Iglič, BMC Vet. Res. 9 (2013) 7.
[7] C. McGuiness, R. Duffin, S. Brown, N.L. Mills, I.L. Megson, W. MacNee, S. Johnston, S.L. Lu, L. Tran, R. Li, X. Wang, D.E. Newby, K. Donaldson, Toxicol. Sci. 119 (2011) 359.
[8] O. Gamucci, A. Bertero, M. Gagliardi, G. Bardi, Coatings 4 (2014) 139.
[9] Q. Jiao, L., Li, Q. Mu and Q. Zhang, Biomed Research International, Article ID 426,028 (2014), doi:10.1155/2014/426028.
[10] B.S. Zolnik, A. González-Fernández, N. Sadriech, M.A. Dobrovolskaia, Endocrinology 151 (2010) 458.
[11] M. Elsabahy, K.L. Wooley, Chem. Soc. Rev. 42 (2013) 5552.
[12] E.M. Walker, S.M. Walker, Ann. Clin. Lab. Sci. 30 (2000) 354.
[13] X.M. Yuan, W. Li, Curr. Med. Chem. 15 (2008) 2157.
[14] S.L. Easo, P.V. Mohanan, Carbohydr. Polym. 92 (2013) 726.
[15] Y.-S. Lin, C.L. Haynes, Chem. Mater. 21 (2009) 3979.
[16] C.D. Goodman, T. Yilmaz, V.M. Rotello, Bioconjug. Chem. 15 (2004) 897.
[17] L.M. Ali, M. Gutiérrez, R. Cornudella, J.A. Moreno, R. Piñol, L. Gabilondo, A. Millán, F. Palacio, J. Biomed. Nanotechnol. 9 (2013) 1272.
[18] S. Passemard, D. Staedler, L. Učňová, G.S. Schneiter, P. Kong, L. Bonacina, L. Juillerat-Jeanneret, S. Gerber-Lemaire, Bioorg. Med. Chem. Lett. 23 (2013) 5006.
[19] S.M. Chowdhury, S. Kanakia, J.D. Toussaint, M.D. Frame, A.M. Dewar, K.R. Shroyer, W. Moore, B. Sitharaman, Sci. Rep. 3 (2013) 2584.
[20] D. Simberg, J.-H. Park, P.P. Karmali, W.-M. Zhang, S. Merkulov, K. McCrae, S. Bhatia, M. Sailor, E. Ruoslahti, Biomaterials 30 (2009) 3926.
[21] K. Saha, D.F. Moyano, V.M. Rotello, Mater Horiz. 1 (2014) 102.
[22] A.J. Paula, D.S.T. Martinez, R.T.A. Júnior, A.G.S. Filho, O.L. Alves, J. Braz. Chem. Soc. 23 (2012) 1807.
[23] S. Deb, S.O. Raja, A.K. Dasupta, R. Sarkar, A.P. Chattopadhyay, U. Chaudhuri, P. Guha, P. Sardar, Blood Cells. Mol. Dis. 48 (2010) 36.
[24] M.A. Pachkam and J.F. Mustard, Circulation, 62 (suppl V) (1980) V26.
[25] P. Robless, D. Okonko, D.P. Mikhailidis, G. Stansby, Platelets 15 (2004) 215.
[26] P. Költringer, W. Langsteger, P. Lind, G. Klima, F. Reisecker, O. Eber, Acta Med. Austriaca 17 (1990) 79.
[27] L.A. Harker, V. Fuster, J. Am. Coll. Cardiol. 8 (1986) 21B.
[28] M. Oberg, U. Hedner, S.-E. Bergentz, Thromb. Res. 12 (1978) 629.
[29] H.J. Weiss, J. Lab. Clin. Med 69 (1967) 37.
[30] S. Hayashi, S. Okamura, C. Kawasaki, M. Harada, Y. Niho, Biomed. Pharmacother. 47 (1993) 155.
[31] M. Krönke, W.J. Leonard, J.M. Depper, W.C. Greene, J. Exp. Med. 161 (1985) 1593.
[32] H.G. Nuesslein, H.L. Spiegelberg, J. Clin. Lab. Anal. 4 (1990) 414.
[33] R.D. Cummings, M.E. Etzler, Essentials of Glycobiology, in: A. Varki, R.D. Cummings, J.D. Esko (Eds.), 2nd edition, Cold Spring Harbor, New York, 2009, Chapter 45.
[34] P.C. Nowell, Cancer Res. 20 (1960) 462.
[35] J.B. Sundstrom, H. Mao, R. Santoianni, F. Villinger, D.M. Little, T.T. Huynh, A.E. Mayne, E. Hao, A.A. Ansari, J. Acquir. Defic. Syndr. 35 (2004) 9.
[36] B. Sojka, M. Kuricova, A. Liskova, M. Bartusova, M. Banski, J. Misiewicz, M. Dusinska, M. Horvathova, E. Jahnova, S. Ilavska, M. Szabova, E. Rollerova, A. Podhorodecki, J. Tulinska, J. Appl. Toxicol. 34 (2014) 1220.
[37] A. Lankoff, M. Arabski, A. Wegierek-Ciuk, M. Kruszewski, H. Lisowska, A. Banasik-Nowak, K. Rozga-Wijas, M. Wojewodzka, S. Slomkowski, Nanotoxicol 7 (2013) 235.
[38] D. Pouliquen, J.J.L. Jeune, R. Perdrisot, A. Ermias, P. Jallet, Magn. Reson. Imaging 9 (1991) 275.
[39] R. Weissleder, D.D. Stark, B.L. Engelstad, B.A. Bacon, C.C. Compton, D.L. White, P. Jacobs, J. Lewis, Am. J. Roentgenol. 152 (1989) 167.
[40] L.L. Estevanato, L.M. Lacava, L.C. Carvalho, R.B. Azevedo, O. Silva, F. Pelegrini, S.N. Báo, P.C. Morais, Z.G. Lacava, J. Biomed Nanotechnol. 8 (2012) 301.
[41] M.G. Krukemeyer, V. Krenn, M. Jakobs, W. Wagner, J. Surg. Res. 175 (2012) 35.
[42] B.-A. Chen, N. Jin, J. Wang, J. Ding, C. Gao, J. Cheng, G. Xia, F. Gao, Y. Zhou, Y. Chen, G. Zhou, X. Li, Y. Zhang, M. Tang, X. Wang, Int. J. Nanomedicine 5 (2010) 593.
[43] C.C. Shen, C.C. Wang, M.H. Liao, T.R. Jan, Int. J. Nanomedicine 6 (2011) 1229.